Effect of Glycerol on Thermal and Mechanical Properties of Polyvinyl Alcohol/Starch Blends

P. A. Sreekumar, Mamdouh A. Al-Harthi, S. K. De

Department of Chemical Engineering, King Fahd University of Petroleum & Minerals, Dhahran 31261, Kingdom of Saudi Arabia

Received 16 January 2011; accepted 2 March 2011
DOI 10.1002/app.34465
Published online 26 July 2011 in Wiley Online Library (wileyonlinelibrary.com).

ABSTRACT: The paper reports the results of studies on the effect of glycerol content on thermal, mechanical, and dynamic mechanical properties of blends of starch and polyvinyl alcohol (PVA). Degree of crystallinity of the starch/PVA blends (4 g/4 g ratio) remains almost constant up to 3.78 g of glycerol as determined by differential scanning calorimetry (DSC) and x-ray diffraction studies. At higher loading of glycerol the crystallinity decreases. DTG thermograms revealed occurring of one maximum degradation temperature closer to that of starch in blends containing up to 3.78 g of glycerol. At higher glycerol content there gradually occur two distinct peaks of maximum degradation temperature, one occurring close to that of starch and other occurring close to the PVA peak, indicating phase separation of the blend components. Results of stress–strain studies indicate lowering of tensile properties and energy at break particularly at higher glycerol content (beyond 3.78 g). Dynamic mechanical studies reveal a sharp drop in dynamic modulus at higher glycerol content at all temperatures. The blend with low glycerol content shows transitions of starch, while the blend containing high glycerol content beyond 3.78 g display the transitions due to both starch and PVA. © 2011 Wiley Periodicals, Inc. J Appl Polym Sci 123: 135–142, 2012

Key words: starch; polyvinyl alcohol; thermal properties; XRD; viscoelastic properties

INTRODUCTION

The use of biodegradable polymers for packaging offers an alternative to the problem of accumulation of solid waste made of synthetic polymers. The low cost and easy availability of starch offers a potential alternative for synthetic polymers in applications where rapid degradation is preferred over long-term durability. The functionality and properties of starch depend mainly on its source, molecular weight, and variation in amylose and amylopectin.

There are reports on the modification of starch to suit different applications.[1,2] Addition of plasticizers such as glycerol, water, and urea-formaldehyde improves the mechanical, thermal, and water absorption properties of starch-based matrices.[3–5] Another method is the blending of starch with other polymers such as polyolefins, polystyrene, poly(vinyl alcohol) (PVA), and poly(lactic acid).[6–12] PVA is water soluble and is an excellent biodegradable polymer and is being used as hydrogels, adhesives, and packing materials.[13,14] Earlier Siddaramaiah et al.[15] investigated the optical, tensile, and burst strength of the polyvinyl alcohol/starch composites. Starch/PVA blends looks promising as biodegradable polymers. The processing of starch/PVA blends can be improved by the incorporation of glycerol.[16] Studies on the modification of the starch/PVA blend using glycerol, citric acid, UV radiation, and plasma treatments have been reported.[17–20]

The present article reports the results of studies on the effect of varying amounts of glycerol on the mechanical, viscoelastic, thermal, and crystallization behavior of the starch/PVA blend at a constant blend ratio.

EXPERIMENTAL

Materials

Corn starch was provided by ARASCO Corn products, Dammam, Saudi Arabia. Glycerol and PVA having molecular weight (M_w) of 27,000 and degree of hydrolysis (98–98.8 mol %) were procured from Sigma Aldrich.

Preparation of blends

Thermoplastic starch based blends were fabricated using solution cast method. Starch, PVA, and glycerol were dissolved in 100 mL of water, according to the formulations in Table I. The mixture was stirred for 45 min at 80°C. After gelation the solution was cast into a glass plate placed on a leveled flat surface. The blends were allowed to dry at 40°C in an

Correspondence to: S. K. De (sadhan@kfupm.edu.sa).

TABLE I
Formulation Used in Preparing the Starch/PVA Blends[a,b]

Blend designation	Glycerol loading, g (ml)
SPG1	1.26 (1 ml)
SPG2	2.56 (2 ml)
SPG3	3.78 (3 ml)
SPG4	5.04 (4 ml)
SPG5	6.30 (5 ml)

[a] Formulation SPG1, SPG2, SPG3, SPG4, and SPG5 consists of 4 g of corn starch and 4 g of PVA in 100 ml water.
[b] Control formulations S contains 8 g of starch and 3.78 g (3 ml)of glycerol in 100 ml water and P contains 8 g of PVA and 3.78 g (3 ml) of glycerol in 100 ml water.

air oven for 16 h. The fully dried membranes were peeled away from the plate and were compressed in a carver press at 120°C for 10 min.

Characterization

FTIR analysis

The IR spectra were obtained using a Thermo NICOLET 6700 FT-IR Spectrometer. Data were collected by averaging 32 scans, at a resolution of 4 cm^{-1} from 500 to 4500 cm^{-1}.

DSC analysis

The melting and crystallization behavior of the blends were determined by using DSC-Q1000, Universal V4.2E TA Instruments. The first heating was done from a temperature of −80 to 200°C at a rate of 10°C/min, followed by isothermal heating for 5 min. First cooling and second heating were performed at 10°C/min in nitrogen atmosphere. Calibrations in DSC were done by measuring the temperature and the enthalpy of melting of indium.

XRD analysis

X-ray diffractometer used was LABX XRD-6000, Shimadzu, Japan. X-rays of 1.5410 A° wavelength was generated by Cu–Kα source. The angle of diffraction, 2θ was varied from 10° to 50° to identify any changes in the crystal structure and intermolecular distances between the intersegmental chains.

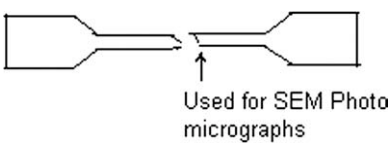

Figure 1 Schematic diagram of the tensile fractured surface used for SEM photomicrographs.

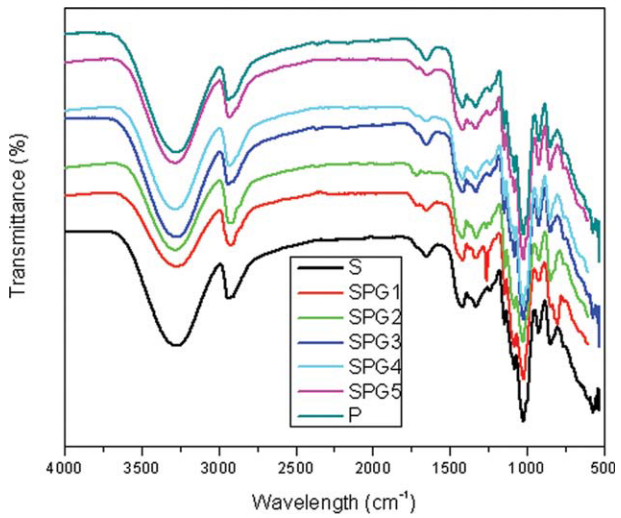

Figure 2 FTIR spectra of starch/PVA blends. [Color figure can be viewed in the online issue, which is available at wileyonlinelibrary.com.]

Thermal stability

Thermal degradation studies were performed by thermogravimetric measurements using TGA-Q500 (TA instruments). Samples weighing approximately 15 mg were heated in nitrogen atmosphere from 25° to 800°C at a heating rate of 10°C/min.

Tensile properties

Tensile tests were carried out by using a universal testing machine (Instron model 5560). The tests were performed according to ASTM D 638-03 standard. Tensile samples were prepared by cutting dumbbell samples from the films by using ASTM Die C. The data presented correspond to the average value of five measurements.

Dynamic mechanical analysis

Dynamic mechanical behavior of materials was studied by using dynamic mechanical analyzer TAQ-800, TA instruments. The experiments were performed under tensile mode at a frequency of 1 Hz at a heating rate of 5°C/min.

Scanning electron micrograph (SEM)

The fractured surfaces of the tensile tested samples (Fig. 1) for the starch/PVA blends were investigated by using a scanning electron microscope JEOL (Model JSM 5800LV). Samples were coated with a thin layer of carbon using a carbon evaporator to avoid sample charging during imaging.

TABLE II
Summary of FTIR Results

Functional group	S (cm^{-1})	SPG1 (cm^{-1})	SPG2 (cm^{-1})	SPG3 (cm^{-1})	SPG4 (cm^{-1})	SPG5 (cm^{-1})	P (cm^{-1})
OH stretching vibrations	3271	3272	3272	3274	3280	3281	3265
C—H stretching	2936	2920	2925	2936	2930	2930	2939
Bound water	1651	1651	1650	1650	1650	1649	1658
Vibrations associated to CH_2 group	1416, 846	1415, 845	1416, 845	1415, 845	1416, 848	1415, 847	843
C—O—C	1328, 1022	1327, 1021	1327, 1021	1331, 1021	1330, 1021	1330, 1021	1325
C—O stretching	1144	1147	1145	1145	1144	1145	1084

RESULTS AND DISCUSSION

The FTIR spectra of representative blends are shown in Figure 2. For all the blends, the strong and broad absorption peaks at 3200–3500 cm^{-1} were assigned to the characteristic absorption peaks of the stretching vibration of —OH of starch units and as well as due to the moisture content. The absorption bands at 2921cm^{-1} refer to the C—H stretching in the starch molecules. The peak at 1651 cm^{-1} corresponds to the bound water indicating the presence of strong hydrogen bonding.[21] The bands located at 1416 cm^{-1} and 846 cm^{-1} are assigned to the vibrations associated with the CH_2 group. The absorptions at 1327 cm^{-1} and 1022 cm^{-1} have been shown to be due to mode involving deformations of C—O—C groups.[21] The C—O stretching mode is related to the band at 1178 cm^{-1}.[22] Details of the

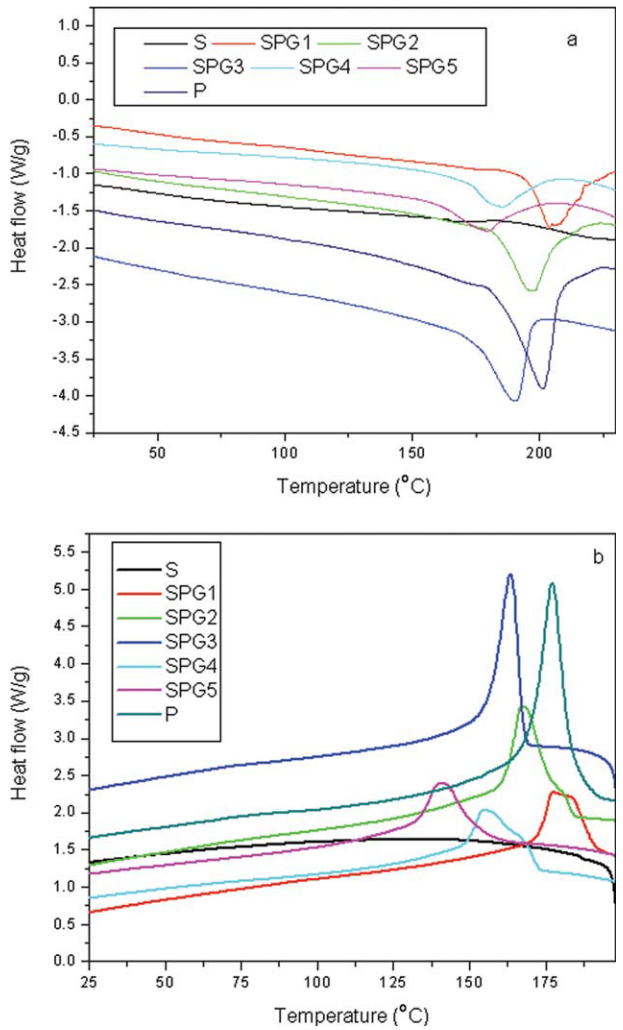

Figure 3 (a) DSC heating curves of starch/PVA blends having different glycerol content. (b) DSC cooling curves of starch/PVA blends having different glycerol content. [Color figure can be viewed in the online issue, which is available at wileyonlinelibrary.com.]

TABLE III
T_{cry}, T_m, ΔH_{Cry}, ΔH_m and Degree of Crystallinity of Starch/PVA Blends

Materials	T_{cry} (°C)	ΔH_{cry} (J/g)	T_m (°C)	ΔH_m (J/g)	Crystallinity (%)
S	–	–	–	–	–
SPG1	177	21.11	204	14.26	21
SPG2	168	22.17	197	15.89	21
SPG3	163	22.96	190	16.38	22
SPG4	154	17.99	185	10.81	15
SPG5	140	14.84	179	7.8	10
P	177	43.03	201	36.53	26

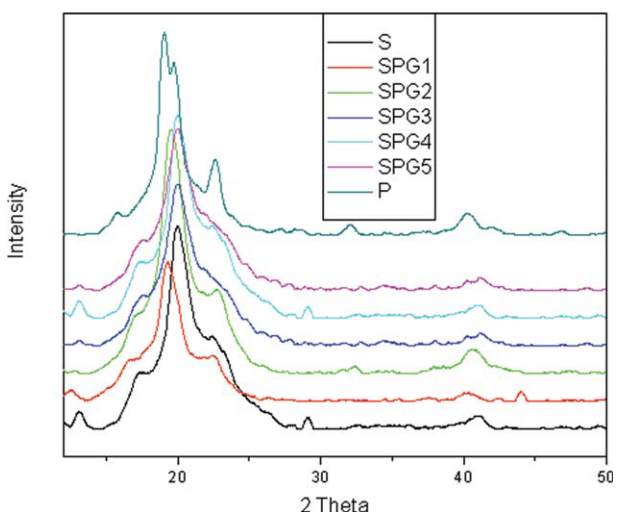

Figure 4 XRD pattern for the starch/ PVA blends. [Color figure can be viewed in the online issue, which is available at wileyonlinelibrary.com.]

TABLE IV
X-Ray Diffraction Parameters and Degree of Crystallinity of Starch/PVA Blends

Material	Angle	D value	FWHM	*I*	Crystallinity (%)
S	17.4000	5.09253	1.8266	138	4
	20.2633	3.96583	2.1267	493	
	22.4000	3.96583	3.1400	227	
SPG1	17.9000	4.94044	0.0000	177	22
	19.5300	4.53973	1.7289	694	
	22.6800	3.91750	1.5600	179	
	40.4655	2.22276	1.5000	63	
SPG2	17.8200	4.97344	0.0000	126	23
	19.4300	4.56388	1.8520	638	
	22.4600	3.95537	1.8134	111	
	40.3100	2.23560	1.2200	21	
SPG3	17.2000	5.15129	2.2900	125	22
	19.4901	4.41847	1.6637	628	
	22.3000	3.81464	0.9688	265	
	40.8483	2.20737	1.2767	60	
SPG4	17.7000	5.2850	1.2266	24	17
	19.6800	4.5070	1.9900	492	
	22.7600	3.9032	2.0400	206	
	40.6700	2.2164	1.6800	60	
SPG5	17.4400	5.08094	1.9200	197	12
	19.1400	4.40456	2.2000	433	
	22.2200	3.99755	0.0000	226	
	40.1600	2.24360	0.6400	22	
P	11.1000	7.9649	0.7000	71	28
	19.7000	4.50285	1.3300	417	
	40.26	2.23826	1.4000	52	

absorption peaks for each blend are summarized in the Table II. It is evident that the addition of glycerol to the blends causes an increase in the intensity as well as a shift in the absorption peak of —OH group from 3271 to 3281 cm^{-1} due to the increase in the intermolecular hydrogen bonding.

Figure 3(a,b) display the DSC thermograms of starch-PVA blend as a function of glycerol concentration. It is evident that all blends show endothermic peaks related to melting of crystallites. The ΔH_m, ΔH_{cry}, T_{cry}, and T_m values along with the percentage of crystallinity for the blends as a function of glycerol content is summarized in Table III. ΔH_{cry}, ΔH_m, and percentage of crystallinity remain almost unchanged up to a glycerol content of 3.78 g, beyond which crystallinity registers a drastic drop. The percentage of crystallinity was calculated using the following expression is shown in Table III.

$$\% \text{ of crystallinity} = (\Delta H_{fus}/\Delta H^0{}_{fus}) \times 100 \quad (1)$$

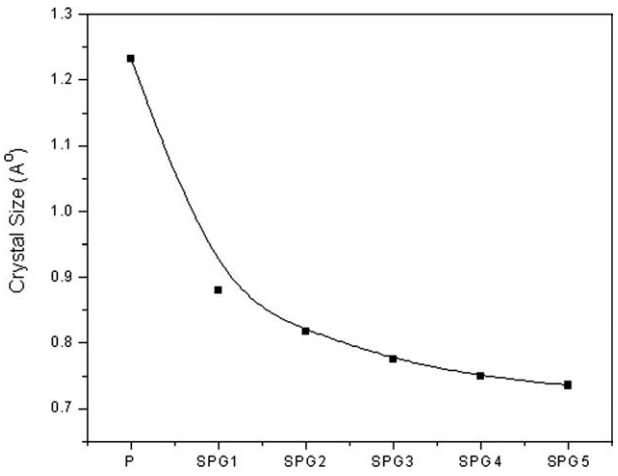

Figure 5 Crystallite size in the starch/PVA blends.

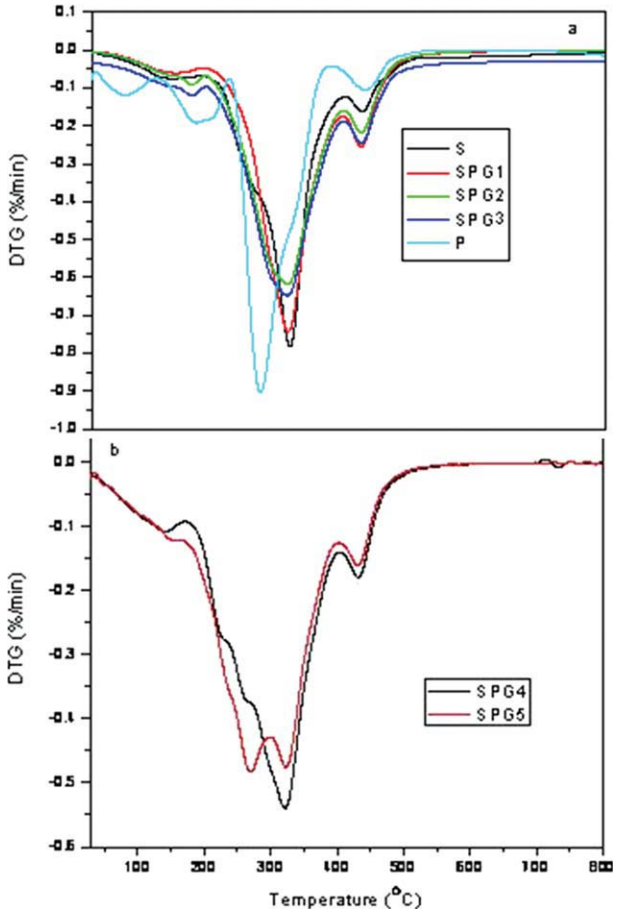

Figure 6 DTG curves of starch/PVA blends. [Color figure can be viewed in the online issue, which is available at wileyonlinelibrary.com.]

TABLE V
Results of TG Studies of the Starch/PVA Blends

Material	Mass loss at 200°C (%)	Maximum degradation temperature (°C)		Residue (%)
		T_{m1}	T_{m2}	
S	8.4	–	326	8.3
SPG1	6.4	–	326	9.8
SPG2	7.8	–	324	8.3
SPG3	11.03	–	323	7.3
SPG4	13.45	267	322	7.1
SPG5	15.26	269	322	6.3
P	21.0	–	285	1.4

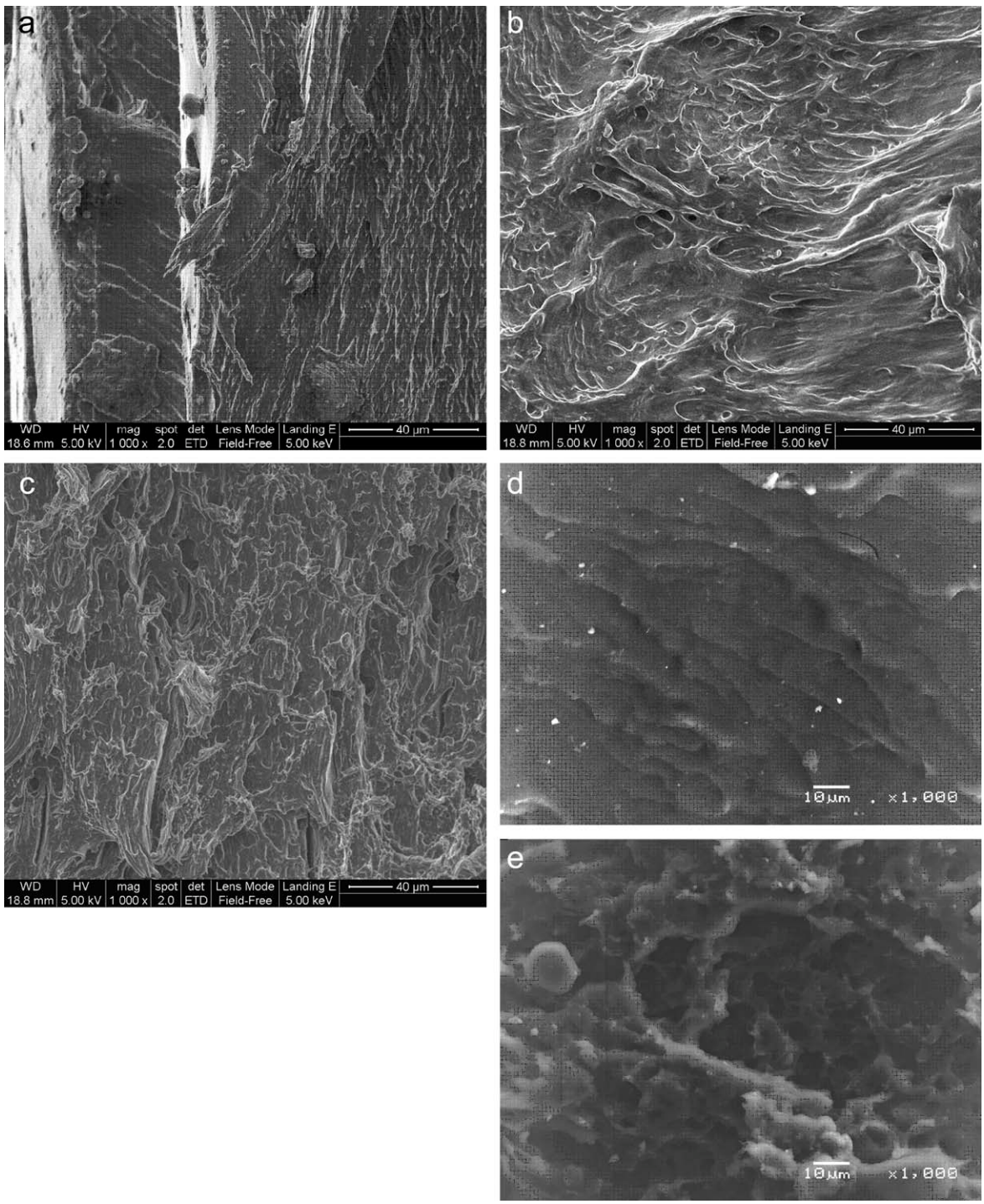

Figure 7 (a) SEM tensile fracto-micrograph of P. (b) SEM tensile fracto-micrograph of SPG1. (c) SEM tensile fracto-micrographs of SPG3. (d) SEM tensile fracto-micrographs of SPG5. (e) SEM tensile fracto-micrographs of S.

where ΔH_{fus} is the enthalpy of fusion of the starch/PVA blend and ΔH^0_{fus} is the enthalpy of fusion of the 100% crystalline PVA. ΔH^0_{fus} of PVA was taken as 141.932 J/g.[23] For example, percentage of crystallinity of the starch/PVA blends remains constant (at 21%) up to the glycerol loading of 3.78 g, beyond which it drops down to 15% at 5.04 g and to 10% at 6.30 g of glycerol content. Results of XRD studies, given below, are in agreement with the results of DSC studies. As has been presented later, results of thermogravimetric studies revealed a phase separation in the blends at higher loading of glycerol resulting in inhomogenity and fall in crystallinity.

The x-ray diffraction pattern of starch/PVA blends at various compositions is given in Figure 4. For the blends the peaks were observed at 11.3, 15.2, 17.9,

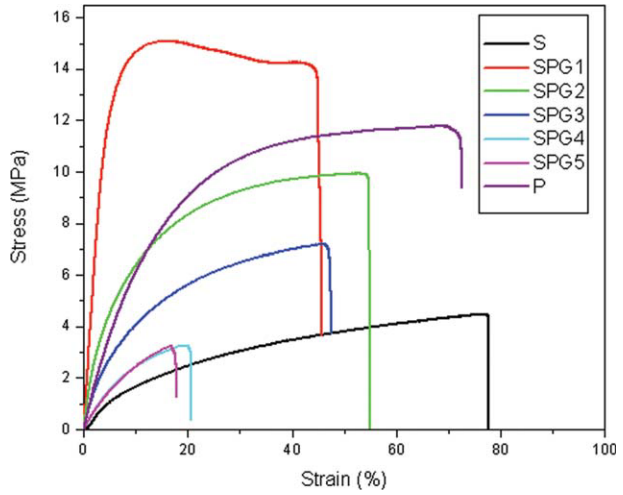

Figure 8 Stress-strain plots for the starch/PVA blends. [Color figure can be viewed in the online issue, which is available at wileyonlinelibrary.com.]

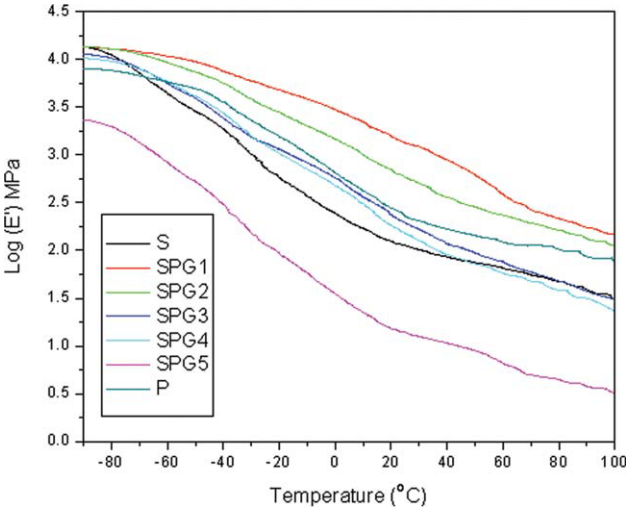

Figure 9 Plots of storage modulus versus temperature of the starch/PVA blends. [Color figure can be viewed in the online issue, which is available at wileyonlinelibrary.com.]

19.5, 22.6, and 40.4°. The peaks observed at 19.5° and 40.4° are the characteristics peaks of PVA, while the peaks for the starch appears at 11.28, 16.2, 17.9, and 22.6°. The intensity of the peak at 19.5° which is the characteristic peak of the PVA decreases on the addition of glycerol. Variation in the *d* values and the intensity of the peaks are given in Table IV. In the starch/PVA blends the reduction in intensity and widening of the peaks indicate that there is a reduction in crystal size. Crystal size was determined by using the following eq. (2)

$$L_{\mathrm{h\,kl}} = \frac{\lambda}{(\mathrm{B}^2 - \mathrm{b}^2)^{1/2}} \cdot \frac{1}{\cos(\theta_{\mathrm{h\,kl}})} \tag{2}$$

where L_{hkl} is the thickness of crystal according to the direction [*h k l*]; θ_{hkl} is the Bragg angle; λ is the wavelength of x-rays; *B* is the width with middle height of the peak characteristic of the planes (*h k l*), and *b* is the corrective term which takes into account the widening of the rays due to the experimental device. This formula is appropriate for crystals of an order of magnitude ranging between 1 and 100 nm. The crystallite size of the samples was calculated with respect to the 19.5° peak of the PVA. Figure 5 represents the variation of crystallite size of PVA as a function of glycerol content. Addition of glycerol to the starch/PVA blend decreases the crystallite size indicating the reduction in the percentage of crystallinity. The degree of crystallinity of samples was quantitatively estimated following the method of Nara and Komiya.[24] A smooth curve which connected peak baselines was computer-plotted on the diffractograms. The area above the smooth curve was taken as the crystalline portion, and the lower area between smooth curve and the linear baseline which connected the two points of the intensity 2θ of 50° and 10° in the samples was taken as the amorphous section. The upper diffraction peak area and the total diffraction area over the diffraction angle 10–50° were integrated using Smadchrom software (Morgan and Kennedy Research, Australia). The ratio of upper area to total diffraction was taken as the degree of crystallinity.

The degree of crystallinity was calculated as follows:

$$X_c = A_c/(A_c + A_a) \tag{3}$$

TABLE VI
Stress-Strain Properties of the Starch/PVA Blends

Material	Tensile strength (MPa)	Young's modulus (MPa)	Elongation (%)	Energy at break (J/m^2)
S	4.35 ± 0.2	22 ± 1	66 ± 0.5	243 ± 11
SPG1	14.6 ± 0.8	429 ± 9	44 ± 1	621 ± 15
SPG2	9.5 ± 0.4	132 ± 4	54 ± 3	446 ± 17
SPG3	7.1 ± 0.3	54 ± 2	52 ± 3	255 ± 17
SPG4	3.0 ± 0.2	34 ± 2	21 ± 2	46 ± 4
SPG5	2.6 ± 0.3	27 ± 3	18 ± 0.6	37 ± 3
P	11.93 ± 0.1	78 ± 2	72 ± 0.1	696 ± 13

TABLE VII
Storage Moduli of Starch/PVA Blends at Different Temperatures

Material	Storage modulus (MPa)		
	0°C	25°C	50°C
S	241	59	25
SPG1	2852	1323	613
SPG2	1442	499	284
SPG3	575	193	85
SPG4	476	149	72
SPG5	35	24	9
P	641	226	93

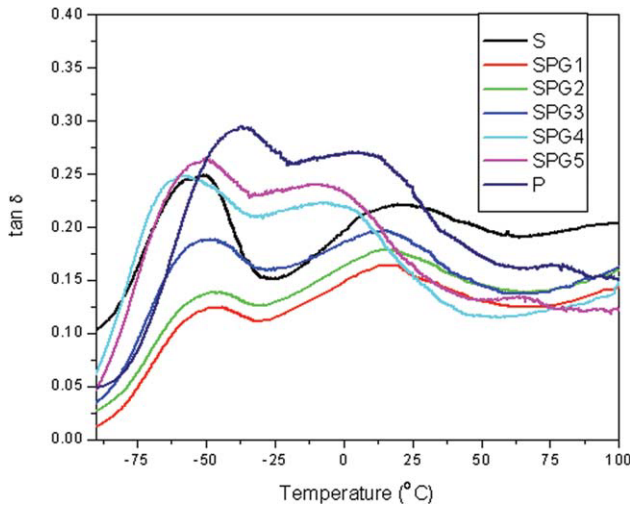

Figure 10 Plots of tan δ versus temperature of the starch/PVA blends. [Color figure can be viewed in the online issue, which is available at wileyonlinelibrary.com.]

where X_c refers to the degree of crystallinity; A_c refers to the crystallized area on the x-ray diffractogram; A_a refers to the amorphous area on the X-ray diffractogram. The percentage of crystallinity calculated is summarized in Table IV. It is evident that the percentage of crystallinity for the blends having glycerol content up to 3.78 g remains almost constant and further increase in the glycerol content causes reduction in the percentage of crystallinity drastically, which is corroborated by the results of DSC analysis.

The DTG curves for starch, PVA, and the blends as a function of glycerol content is given in Figure 6(a,b). For the blends the mass loss occurs in three stages in the temperature zones of 200°C; 200–350°C, and 350–500°C. The initial mass loss below 200°C is due to the evaporation of liquids (that is, water and glycerol).[25] The mass loss varies according to the glycerol content. In the second stage (i.e., in the range 200–350°C) the main degradation occurs. Addition of glycerol to the starch/PVA blend decreases the maximum degradation temperature from 326 to 322°C at 5.04 g and the residual mass from 9.8 to 7% w/w (Table V). This decrease in the thermal stability of the blends is due to the plasticization effect of glycerol. However, it is interesting to note that the DTG thermograms of the blends; namely SPG1, SPG2, and SPG3 are similar to that of starch displaying one peak for the maximum degradation.[26] But the other two blends (that is, SPG4 and SPG5) containing high glycerol content register two degradation peak temperatures one occurring close to starch while the other close to PVA, which are characteristic of immiscible polymer blends.[27] This effect is more prominent in the blend SPG5. This shows that the blend homogeneity decreases above 3.78 g of glycerol, which is also corroborated by the representative SEM fractographs [Fig. 7(a–e)]. Blends SPG1 and SPG3 [Fig. 7(b,c)] show characteristics similar to PVA [Fig. 7(a)], while SPG5 shows characteristics similar to starch [Fig. 7(e)].

Stress–strain plots of the blends are shown in Figure 8 and the results are summarized in Table VI. The tensile strength and Young's modulus of the starch/PVA blends decrease with increase in the glycerol content. But the decrease is very sharp as glycerol content increases beyond 3.78 g and the ductility of the blends drops sharply. Similar results have been obtained by Saiah et al.[28] in the case of thermoplastic thin films based on wheat flour.

Figure 9 displays the variation in storage modulus of the starch-PVA blends as a function of glycerol loading and the results are summarized in the Table VII. The storage modulus decreases with increase in the glycerol content of the blend which is attributed to the plasticization effect of glycerol. The tan δ versus temperature plots for the blends are shown in Figure 10. The blends, except SPG5, display two transitions; one in the low temperature region (around −52°C) and the other in the high temperature region (between 11 and 16°C). Temperature at tan δ_{max1} remains almost constant at different glycerol contents and is close to that of formula S (starch). However, the temperature corresponding to tan δ_{max2} decreases gradually and in the case of SPG5 at the glycerol loading of 6.30 g, the

TABLE VIII
Values of Tan δ_{max} and Temperature at Tan δ_{max} for the Starch/PVA Blends

	1st Transition		2nd Transition		3rd Transition	
Material	Tan δ_{max1}	Temperature at tan δ_{max1} (°C)	Tan δ_{max2}	Temperature at tan δ_{max2} (°C)	Tan δ_{max3}	Temperature at tan δ_{max3} (°C)
S	0.24	−52	0.22	18	–	–
SPG1	0.12	−53	0.16	16	–	–
SPG2	0.13	−52	0.17	14	–	–
SPG3	0.18	−51	0.19	14	–	–
SPG4	0.24	−51	0.18	11	–	–
SPG5	0.26	−51	0.24	−7	0.13	59
P	0.28	−47	0.26	−9	0.16	72

temperature of tan δ_{max2} is closer to that of PVA and this is followed by another high temperature transition (tan δ_{max3}) at 59°C. The behavior of blend SPG5 shows the inhomogeneity in the blend morphology registering transitions for both starch and PVA and the phenomena is displayed to a lesser extent in the case of blend SPG4.

CONCLUSIONS

(1). The crystallinity of starch/PVA blends drops at higher loading of glycerol.
(2). The blend constituent becomes phase separated at high loadings of glycerol which is corroborated by the results of DTG thermograms, stress-strain properties and DMA studies.
(3). In the 4 g/4 g starch PVA blend, maximum of 3.78 g (3 mL) of glycerol can be used without causing sharp drop in the ductility, mechanical, and dynamic mechanical properties.

References

1. Reddy, N.; Yiqi, Y. Food Chem 2010, 118, 702.
2. Saiah, R.; Sreekumar, P. A.; Leblanc, N.; Castandet, M.; Saiter, J M. Indus Crops Prod 2009, 29, 241.
3. Westling, A. R.; Stading, M.; Hermansson, A. M.; Gatenholm, P. Carbohydr Polym 1998, 36, 217.
4. Follain, N.; Joly, C.; Dole, P.; Roge, B.; Mathlouthi, M. Carbohydr Polym 2006, 63, 400.
5. Poutanen, K.; Forssell, P. Trend Polym Sci 1996, 4, 128.
6. Prachayawarakorn, S. P.; Boonpasith, P. Carbohydr Polym 2010, 81, 425.
7. Chiu, F. C.; Lai, S. M.; Ti, K. T. Polym Test 2009, 28, 243.
8. Aurélie, T.; Huneault, M. A.; Favis, B. D. Polymer 2009, 50, 5733.
9. Schlemmer, D.; Sales, M. J. A.; Resck, I. S. Carbohydr Polym 2009, 75, 58.
10. Xiong, H. G.; Tang, S. W.; Tang, H. L.; Zou, P. Carbohydr Polym 2008, 71, 263.
11. Yoon, S. D.; Chough, S. H.; Park, H. R. J Appl Polym Sci 2007, 106, 2485.
12. Fang, Q.; Hana, M. A. Cereal Chem 2000, 77, 779.
13. Lee, J. A.; Kim, M. N. Polym Degrad Stab 2003, 81, 303.
14. Lopez, O. B. L.; Mejia, G. A. I.; Sierra, G. L. Polym Eng Sci 1999, 39, 1346.
15. Siddaramaiah, R. B.; Somashekar, R. J Appl Polym Sci 2004, 91, 630.
16. Wang, J.; Lu, Y.; Yuan, H.; Peng, D. J Appl Polym Sci 2008, 110, 523.
17. Follaina, N.; Joly, C.; Dole, P. C.; Bliard, C. Carbohydr Polym 2005, 60, 185.
18. Park, H. R.; Chough, S. H.; Yun, Y. H.; Yoon, S. D. J Polym Environ 2005, 13, 375.
19. Khan, M. A.; Bhattacharia, S. K.; Kader, M. A.; Bahari, K. Carbohydr Polym 2006, 63, 500.
20. Yang, S. Y.; Liu, C. I.; Wu, J. Y.; Kuo, J. C.; Huang, C. Y. Macromol Symp 2008, 272, 150.
21. Wolkers, W. F.; Oliver, A. E.; Tablin, F.; Crowe, J. H.; Carbohydr Res 2004, 339, 1077.
22. Pavloic, S.; Brandao, P. R. G. Miner Eng 2003, 16, 1117.
23. Nishio, Y.; Tatsuo, H.; Toshisada, T. Macromolecules 1989, 22, 2547.
24. Nara, S.; Komiya, T. Starch-Starke 1983, 35, 407.
25. Leblanc, N.; Saiah, R.; Beucher, E.; Gattin, R.; Castandet, M.; Saiter, J. M. Carbohydr Polym 2008, 73, 548.
26. Sircar, A. K.; Lamond, T. G. Rubb Chem Technol 1975, 48, 640.
27. Bikales, N. M. Characterization of Polymers; Wiley-Interscience: New York, 1971.
28. Saiah, R.; Sreekumar, P. A.; Leblanc, N.; Castandet, M.; Saiter, J. M. Cereal Chem 2007, 84, 276.